GRANMA manuscript No.
(will be inserted by the editor)

A micromechanical model of collapsing quicksand

Dirk Kadau[1], José S. Andrade Jr.[2] and Hans J. Herrmann[1,2]

arXiv:1012.2696v1 [cond-mat.soft] 13 Dec 2010

Abstract The discrete element method constitutes a general class of modeling techniques to simulate the microscopic behavior (i.e. at the particle scale) of granular/soil materials. We present a contact dynamics method, accounting for the cohesive nature of fine powders and soils. A modification of the model adjusted to capture the essential physical processes underlying the dynamics of generation and collapse of loose systems is able to simulate "quicksand" behavior of a collapsing soil material, in particular of a specific type, which we call "living quicksand". We investigate the penetration behavior of an object for varying density of the material. We also investigate the dynamics of the penetration process, by measuring the relation between the driving force and the resulting velocity of the intruder, leading to a "power law" behavior with exponent 1/2, i.e. a quadratic velocity dependence of the drag force on the intruder.

Key words. Granular matter, Contact Dynamics Simulations, Distinct Element Method, Quicksand, Collapsible soil, Biomaterial

1 Introduction

Despite the ubiquitous appearance of quicksand in adventure books and movies, its origin and physico-chemical behavior still represent controversial scientific issues in the fields of soil and fluid mechanics [1,2,3,4,5]. It has been argued repeatedly [6] that, because the density of sludge is typically larger than that of water, a person cannot fully submerge, and therefore cannot be really "swallowed" by any quicksand.

The fluidization of a soil due to an increase in ground water pressure, which in fact is often responsible for catastrophic failures at construction sites, is called by engineers the "quick condition" [7,8], and has been studied extensively up to now [9,10,11]. Another source of fluidization can be vibrations either from an engine [12] or through an earthquake [3]. While this "liquefaction" or "cyclic mobility" phenomenon [13,14,15] can essentially happen with any soil [16], it is known that samples taken from natural quicksand usually show quite specific, but anomalous rheology depending on the peculiarities of the material composition and structure [17]. Also in dry quicksand [18,19] a fragile/metastable structure leads to interesting material behavior like collapse and jet formation after impact of an intruder, although the microscopic material properties are obviously quite different. Nevertheless, wet and dry quicksand are more similar than one would think. Based on results of real and *in situ* quicksand measurements we develop and numerically solve a modified version of the previously presented simulation of a simple physical model for this quicksand/collapsing soil. Here, we focus on the penetration behavior of an intruder.

February 5, 2022

Dirk Kadau, José S. Andrade Jr. and Hans J. Herrmann

Institute for Building Materials, ETH Hönggerberg, 8093 Zürich, Switzerland
Departamento de Física, Universidade Federal do Ceará, 60451-970 Fortaleza, Ceará, Brazil

Correspondence to: dkadau@ethz.ch

2 Experiments and Model

Our physical model is inspired by in situ measurements performed with a specific type of natural quicksand at the shore of drying lagoons located in a natural reserve called Lençois Maranhenses in the North-East of Brazil [20,21, 22,23]. Cyanobacteria form an impermeable crust, giving the impression of a stable ground. After breaking the crust a person rapidly sinks to the bottom of the field. We measured the shear strength of the material before and after perturbation and found a drastic difference. Our measurements indicate that the quicksand is essentially a collapsing suspension with depth independent shear strength. After the collapse, it becomes a soil dominated by the Mohr-Coulomb friction criterion for its shear strength. The material undergoes a cross-over from a yield stress material, i.e. a more fluid-like behavior to a Coulomb material, i.e. more solid-like behavior after the collapse. We would like to point out that the collapse of the metastable structure is irreversible, as opposed to quicksand described in Ref. [17]. In summary, the "living quicksand" studied here can be described as a suspension of a tenuous granular network of cohesive particles. If perturbed, this unusual suspension can drastically collapse, promoting a rapid segregation from water, to irreversibly bury an intruding object.

To model the complex behavior found in the experiments we use a variant of contact dynamics, originally developed to model compact and dry systems with lasting contacts [24,25]. The absence of cohesion between particles can only be justified in dry systems on scales where

the cohesive force is weak compared to the gravitational force on the particle, i.e. for dry sand and coarser materials, which can lead to densities close to that of random dense packings. However, an attractive force, e.g. due to capillary bridges or van der Waals forces, plays an important role in the stabilization of large voids [26], leading to highly porous systems as e.g. in fine cohesive powders, in particular when going to very small grain diameters. Also for contact dynamics a few simple models for cohesive particles have been established [27,28,26]. Here we consider the bonding between two particles in terms of a cohesion model with a constant attractive force F_c acting within a finite range d_c, so that for the opening of a contact a finite energy barrier $F_c d_c$ must be overcome. In addition, we implement rolling friction between two particles in contact, so that large pores can be stable [26,29,30,31,32].

In the case of collapsing "living quicksand" our cohesion model has to be modified. One also has to take into account the time necessary for bonds to appear, i.e. during relatively fast processes new bonds will not be formed, whereas during longer times bonds are allowed to form at a particle contact. Finally, gravity also cannot be neglected in the model since the particle diameter is usually well above the micron-size. For simplicity, however, the surrounding pore water is not explicitly considered but only taken into account as a buoyant medium, reducing the effective gravity acting onto the grains. Disregarding the interstitial fluid motion keeps the model as simple as possible and nevertheless able to reproduce the main experimental observations [21]. The details of the collapse, however, may be influenced by the flow field of the surrounding fluid [19,33]. Testing the influence of the fluid by introducing a viscous drag onto the grains considering water and the typical grain sizes from the experiments showed no significant difference [22,23]. As previously discussed, we justify the cohesive bonds in this case as being mediated by the bacteria living in the suspension.

Summarizing, we use the following contact laws for the simulations presented in this paper. Perfect volume exclusion (Signorini condition) is assumed in normal direction, where a cohesive force is added as described above. In tangential direction Coulomb friction is applied (Coulomb law). Additionally, for the contact torques rolling friction is applied as a threshold law similar to the Coulomb law. A detailed description of this model can be found in Ref. [26]. For the simulation of the collapsing living quicksand the formation and breakage of cohesive bonds has to be considered additionally. Our physical model is validated with the real data obtained from the situ measurements, specifically by comparing the shear strength behavior showing a drastic change when soil was perturbed and the penetration behavior described in more detail in Refs. [20,21, 22].

3 Results

The penetration behavior of our collapsing "living quicksand" has been studied previously for one specific density [20,21,22,23] and is here only briefly summarized. The penetration causes the partial destruction of the porous network and the subsequent compaction of the disassembled material. We observe the creation of a channel which finally collapses over the descending intruder. At the end of the penetration process the intruder is finally buried under the loose debris of small particles. Furthermore, our simulations indicate that in the worst condition, when the cohesive force is completely restored, one could need a force up to three times one's weight to get out of such morass [22]. In this paper we will focus on the penetration process for varying densities while keeping the cohesive force constant.

When creating fragile structures by ballistic deposition and settling due to gravity the density is determined by the strength of the cohesive force. Here we will show a way of generating fragile structures with determined density (within a given range). The particles are deposited ballistically, and settle due to gravity. After the settlement of all particles, the cohesive forces between them are tuned to the point in which a barely stable structure of grains is assured. This results in a tenuous network of grains, like in a house of cards (see fig. 1a), giving the maximal possible density for this specific configuration. In the case shown the volume fraction is 0.441. For different configurations (different seed for the random number generator), used for later averaging, this maximal volume fraction has values ranging from 0.428 to 0.451.

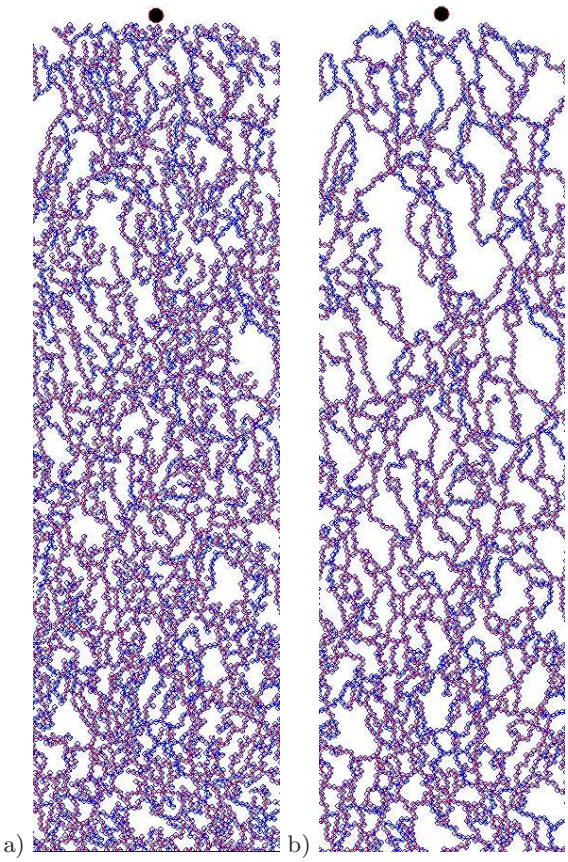


Fig. 1. Maximal density of a configuration after settling without change (a) and minimal density after removing all possible loose ends (b).

For averaging we need configurations with the same initial density. How can we create such structures? Due to the ballistic deposition there are many loose ends in the structure, which do not carry any load. When elimination those loose ends successively one can reduce the density to a given value. This eliminating procedure will be briefly discussed in more detail. Particles with only one contact are not contributing to the force network carrying the weight of the material. Thus, these particles can be eliminated without leading to a collapse of the structure. We check for each particle (in random order) if they have only one contact in which case we eliminate the particle. After we went through all the particles we start again checking all particles, as there will be new particles with coordination number one due to the elimination of a former neighboring particle. This can be done until one reaches a state where no loose ends are present any more. This defines the minimal possible density for a specific configuration as shown in fig. 1b, with volume fraction 0.344 for this specific case. For different configurations this minimal volume fraction ranges from 0.327 to 0.35. This process can be interrupted when a desired density is reached.

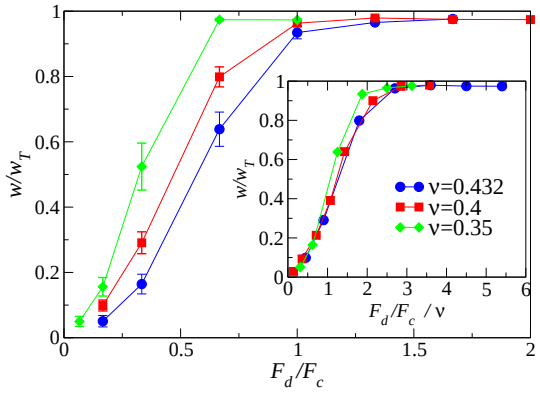


Fig. 2. Penetration depth here measured by the weight w of all grains above the intruder, i.e. larger vertical position, normalized by the total weight w_T) depending on the force F_d acting on the intruder (normalized by cohesive force F_c) for different initial densities of the material. (Connecting lines are shown here for different curves to be better distinguishable.) Inset: Scaling the force axis by the volume fraction of the initial configuration leads to a relatively good collapse for low values of F_d. For higher forces the curves show small deviations due to inertial effects.

Fig. 2 shows the penetration depth depending on the applied force for different densities of the initial configuration. Reducing the density the threshold, needed for pushing in the intruder, reduces, as one expects. Scaling the force with the density, i.e. dividing the x-axis by the volume fraction leads to a data collapse for small forces only (Fig. 2, inset). In this regime where the intruder is relatively slow, the density fully determines how deep the intruder can be pushed in. For higher forces the collapse gets worse due to inertial effects. In this region a better collapse could be achieved when scaling with the square of the density. The influence of inertia can be understood as follows: Structures with larger densities strongly hinder the motion of the intruder. Thus, inertial effects are less effective for these structures, leading to lower penetration depth within these structures.

When looking in more detail at the dynamics of the penetration process it can be seen that, after an initial phase, the velocity fluctuates around a constant value (not shown here) before finally decelerating to zero at the final intruder position, i.e. at the bottom, or at intermediate values. For different forces applied on the intruder these

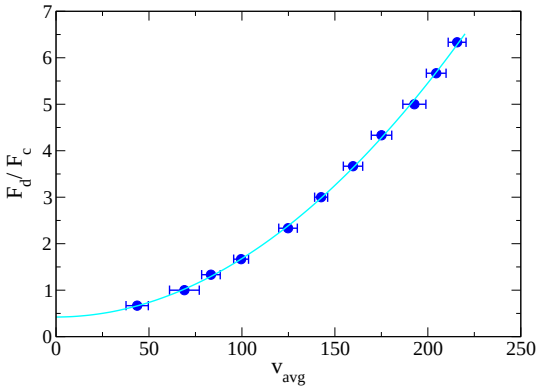


Fig. 3. Relation between applied force and measured average velocity when pushing downwards at one specific density ($\nu = 0.432$). A parabolic fit represents the data quite well.

average velocities can be measured. The relation between the applied force and the measured velocity can be fitted by a quadratic function (fig. 3), where the minimum of the parabola is very close to $v_{\rm avg} = 0$. Alternatively, this minimum can be fixed at $v_{\rm avg} = 0$ leading to an almost identical fitting curve. Summarizing, we found:

$$F_d - F_{\rm thr} \propto v_{\rm avg}^2 \tag{1}$$

In this case the value for $F_{\rm thr}/F_c$ is around 0.42 which is in accordance to the value one could estimate from the force dependence of the relative weight w/w_T above the intruder after penetration. Let us consider the applied force to equalize the drag force on the intruder exerted by the surrounding "complex fluid". The results indicate a yield-stress fluid behavior as also found in shear strength measurements [22,23]. Future rheological measurements could define the specific rheological model. A square velocity dependence of the drag force usually implies that inertia effects are important. Here, the intruder has to accelerate the grains as they are pushed downwards within the compaction process. On the other hand, the force is also needed to break cohesive bonds. The fact that we do not find a viscous like behavior (linear in velocity) agrees with the non-reversibility of the system.

A link can be drawn to the pinning-depinning transition for a force driven interface where the driving force F_d has to overcome a threshold $F_{\rm thr}$ leading to a power law:

$$v \propto (F_d - F_{\rm thr})^\theta \tag{2}$$

The former quadratic behavior previously observed would lead to an exponent $\theta = 1/2$. The results obtained for

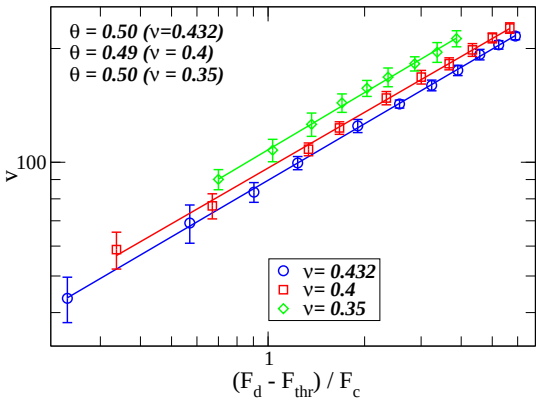


Fig. 4. When plotting the average velocity versus the applied driving force F_d minus a threshold force $F_{\rm thr}$, a power law fit has an exponent of around 1/2 for the three different investigated volume fractions.

different densities are shown in fig.4. Note that one has to determine $F_{\rm thr}$ by adjusting to the optimal power law behavior, then a power law fit estimates the exponent. This procedure gives some additional information about the error of $F_{\rm thr}$ and θ. In the cases presented here varying $F_{\rm thr}$ by about 5% still showed relatively good power laws leading to changing the exponent by less than 5% which also serves here to determine the error of the exponents (instead of the lower value obtained by the statistical analysis by the regression). The values for the exponents are 0.5 ± 0.02 (for $\nu = 0.43$ and $\nu = 0.35$) and 0.49 ± 0.02 (for $\nu = 0.4$). Obviously for all densities the exponent agrees very well with 1/2, suggesting a quadratic dependence on the drag force acting on the intruder.

4 Conclusion

We investigated the density dependence of the penetration behavior of a model for collapsing "living quicksand". We could achieve a data collapse for small forces when plotting the penetration depth depending on the applied force divided by the density. For higher forces or penetration depth inertial effects are important and the scaling is less pronounced. During the penetration process the intruder velocity fluctuates around a constant value except for the very initial acceleration and the final deceleration. This constant velocity shows a power law with exponent $\theta = 1/2$ as function of the driving force minus a threshold force. This means that the drag force on the intruder shows a quadratic velocity dependence. Here the drag force is the driving force shifted by a threshold force.

5 Acknowledgement

We are deeply indebted to Ioannis Vardoulakis for his generosity in sharing his ideas and the inspiring discussions about this subject. We thank CNPq, CAPES, FUNCAP and the PRONEX-CNPq/FUNCAP grant for financial support.

References

1. H. Freundlich and F. Juliusburger. Quicksand as a thixotropic system. *T. Faraday Soc.*, 31:769–773, 1935.
2. G. H. Matthes. Quicksand. *Scientific American*, 188:97–102, 1953.
3. K. Kruszelnicki. And the earth did swallow them up! *New Scientist*, 152:26–29, 1996.
4. L. Bahlmann, S. Klaus, M. Heringlake, W. Baumeier, P. Schmucker, and K. F. Wagner. Rescue of a patient out of a grain container: the quicksand effect of grain. *Resuscitation*, 53:101–104, 2002.
5. S. Yamasaki. What is quicksand? *Sci. Am.*, 288:95–95, 2003.
6. E. R. Smith. The lifting effect of quicksand. *Ohio J. Sci.*, 46:327–328, 1946.
7. R. F. Craig. *Soil Mechanics*. E & FN Spon, New York, 1997.
8. U. El Shamy and M. Zeghal. Coupled continuum-discrete model for saturated granular soils. *Engrg. Mech.*, pages 413–426, 2005.
9. I Vardoulakis. Shear-banding and liquefaction in granular-materials on the basis of a Cosserat continuum theory. *Ingenieur Archiv*, 59(2):106–113, 1989.
10. I Vardoulakis. Fluidisation in artesian flow conditions: Hydromechanically unstable granular media. *Geotechnique*, 54(3):165–177, 2004.
11. I Vardoulakis. Fluidisation in artesian flow conditions: Hydromechanically stable granular media. *Geotechnique*, 54(2):117–130, 2004.
12. D. A. Huerta, V. Sosa, M. C. Vargas, and J. C. Ruiz-Suarez. Archimedes' principle in fluidized granular systems. *Phys. Rev. E*, 72:031307, 2005.
13. G. Castro. Liquefaction and cyclic mobility of saturated soils. *J. of the Geotech. Eng. Div.*, 101:551–569, 1975.
14. K. Ishihara. Liquefaction and flow failure during earthquakes. *Geotechnique*, 43:351–415, 1993.
15. M. Pastor, O. C. Zienkiewicz, and A. H. C. Chan. Generalized plasticity and the modelling of soil behaviour. *Int. J. for Num. and Analyt. Meth. in Geomech.*, 14, 1990.
16. T. W. Lambe and R. V. Whitman. *Soil Mechanics*. Wiley, New York, 1969.
17. A. Khaldoun, E. Eiser, G.H. Wegdam, and D. Bonn. Liquefaction of quicksand under stress. *Nature*, 437:635–635, 2005.
18. D. Lohse, R. Rauhe, R. Bergmann, and D. van der Meer. Creating a dry variety of quicksand. *Nature*, 432:689–690, 2004.
19. J.R. Royer, E.I. Corwin, A. Flior, M.-L. Cordero, M.L. Rivers, P.E. Eng, and Jaeger H.M. Formation of granular jets observed by high-speed x-ray radiography. *Nature Physics*, 1(3):164–167, 2005.
20. D. Kadau, H.J. Herrmann, J.S. Andrade, A.D. Araújo, L.J.C. Bezerra, and L.P. Maia. Living quicksand. *Granular Matter*, 11:67–71, 2009.
21. D. Kadau, H.J. Herrmann, and J.S. Andrade. Mechanical behaviour of "living quicksand": simulation and experiment. In M. Nakagawa and S. Luding, editors, *Powders and Grains 2009*, volume 1145 of *AIP Conference Proceedings*, pages 981–984. Amer. Inst. Physics, 2009.
22. D. Kadau, H.J. Herrmann, and J.S. Andrade. Collapsing granular suspensions. *Eur. Phys. J. E*, 30:275–281, 2009.
23. D. Kadau. From powders to collapsing soil/living quicksand: Discrete modeling and experiment. In P. Giovine

J. D. Goddard, J. T. Jenkins, editor, *IUTAM-ISIMM Symposium on Mathematical Modeling and Physical Instances of Granular Flows*, volume 1227 of *AIP Conf. Proc.*, pages 50–57. Amer. Inst. Physics, 2010.

24. J. J. Moreau. Some numerical methods in multibody dynamics: application to granular materials. *Eur. J. Mech. A-Solid*, 13:93–114, 1994.
25. M. Jean and J. J. Moreau. Unilaterality and dry friction in the dynamics of rigid body collections. In *Contact Mechanics International Symposium*, pages 31–48, Lausanne, 1992. Presses Polytechniques et Universitaires Romandes.
26. D. Kadau, G. Bartels, L. Brendel, and D. E Wolf. Pore stabilization in cohesive granular systems. *Phase Transit.*, 76:315–331, 2003.
27. A. Taboada, N. Estrada, and F. Radjai. Additive decomposition of shear strength in cohesive granular media from grain-scale interactions. *Phys. Rev. Lett.*, 97:098302, 2006.
28. V. Richefeu, M.S. Youssoufi, and E. Azema et al. Force transmission in dry and wet granular media. *Powder Technology*, 190:258–263, 2009.
29. D. Kadau, L. Brendel, G. Bartels, D.E. Wolf, M. Morgeneyer, and J. Schwedes. Macroscopic and microscopic investigation on the history dependence of the mechanical properties of powders. *Chemical Engineering Transactions*, 3:979–984, 2003.
30. G. Bartels, T. Unger, D. Kadau, D.E. Wolf, and J. Kertész. The effect of contact torques on porosity of cohesive powders. *Granular Matter*, 7:139–143, 2005.
31. L. Brendel, D. Kadau, D.E. Wolf, M. Morgeneyer, and J. Schwedes. Compaction of cohesive powders: A novel description. *AIDIC Conference Series*, 6:55–65, 2003.
32. M. Morgeneyer, M. Röck, J. Schwedes, L. Brendel, D. Kadau, D.E. Wolf, and L.-O. Heim. Compaction and mechanical properties of cohesive granular media. *Schriftenreihe Mechanische Verfahrenstechnik: Behavior of Granular Media*, 9:107–136, 2006.
33. G. Caballero, R. Bergmann, D. van der Meer, A. Prosperetti, and D. Lohse. Role of air in granular jet formation. *Phys. Rev. lett.*, 99:018001, 2007.